Journal of Chromatography, 186 (1979) 25–35

CHROM. 12,058

HIGH-PERFORMANCE GAS CHROMATOGRAPHIC COLUMNS PACKED WITH MICRO-PARTICLES

LU PEICHANG, ZHOU LIANGMO, WANG CHINGHAI, WANG GUANGHUA, XIA AIZU and XU FANGBAO

Dalian Institute of Chemical Physics, Chinese Academy of Sciences, Dalian, Liaoning (People's Republic of China)

SUMMARY

The effect of carrier gas and mean particle size on column efficiency in terms of HETP was investigated. When a stainless-steel column (10 cm × 2 mm I.D.) packed with 7 ± 2 μm amorphous silica was used, an $(HETP)_{min.}$ value of 22 μm was obtained, corresponding to $4.5 \cdot 10^4$ theoretical plates per metre and a reduced plate height of 3.1. With this column, the overall mass transfer between two phases is very fast; the rate coefficient of mass transfer calculated from the $\bar{H}\alpha_0$ *versus* $\alpha^2{}_0$ curve was less than 10^{-5} sec.

THEORETICAL

A uniformly packed column may be considered as a bundle of micro-capillaries, arranged at random, through each of which the flow profile of the carrier gas follows a laminar distribution, so that a stagnant interstitial space may exist at the boundary of the two phases. If the equilibrium is instantaneous in the stagnent interstititial space and the mean linear velocity of the carrier gas at each cross-section of a column can also be expressed statistically by α, then according to our early work[1–3], the height equivalent to a theoretical plate ($\bar{H}$ or HETP) may be expressed as

$$\bar{H} = \left(\frac{2\gamma D_{g0}}{\alpha_0} + \frac{\beta^2 d_p^2}{D_{g0}}\alpha_0\right) f_2 + \frac{2}{3} \cdot \frac{k' d_f^2}{(1+k')^2 D_l} \cdot \alpha_0 f_3 + \frac{2kk'}{k_g \sigma (1+k')^2} \cdot \alpha_0 f_3 \quad (1)$$

where

$$f_2 = \frac{9}{8} \cdot \frac{(p^4-1)(p^2-1)}{(p^3-1)^2} \quad (2)$$

$$f_3 = \frac{3}{2} \cdot \frac{(p^2-1)}{(p^3-1)} \quad (3)$$

$$p = p_i/p_0 \quad (4)$$

In the limiting case, when the resistance of the liquid and the interfacial mass transfer are comparatively unimportant, we can thus set $d\bar{H}/d\alpha_0 = 0$ and readily obtain $\bar{H}_{min.}$ and $(\alpha_0)_{opt.}$ as follows:

$$(\alpha_0)_{opt.} = \frac{2\sqrt{\gamma}}{\beta d_p} \cdot D_{g0} \tag{5}$$

$$\bar{H}_{min.} = 2\sqrt{\gamma}\,\beta f_2 d_p \approx 1.6 f_2 d_p \tag{6}$$

It appears that when the liquid and interfacial mass transfer resistance can be ignored, then the theoretical plate height decreases linearly with the mean particle size.

Meyers and Giddings[4] investigated columns packed with micro-particles and obtained 12,400 theoretical plates per metre when 13 ± 2.9 μm modified alumina beads were used. More recently, Huber *et al.*[5], Kenji[6], Di Corcia and co-workers[7,8] and others carried out considerable work on columns packed with micro-particles. The maximum number of theoretical plates per metre obtained was 17,000 by Di Corcia and co-workers using 20–25 μm modified graphitized carbon black. Much progress is currently being made in developing highly efficient columns in both liquid and gas chromatography[9].

The aim of this work was to study the behavior of such a column packing with an even smaller particle size and the effect of the mobile phase on the column efficiency.

EXPERIMENTAL

Apparatus, column and column packings

All experiments were carried out on a home-made gas chromatograph equipped with a flame-ionization detector (FID) with an XWC-200 recorder and an SC-16 oscilloscope to follow the elution peaks. Four grades of YWG silica produced by the Tsingtao Ocean Chemical Plant and Tienjin Secondary Chemical Reagents Plant were used as packing materials. They were YWG 7 (amorphous silica, particle size 7 ± 2 μm); YWG-CN (silica micro-beads bonded with cyano groups, particle size range 10–15 μm); YWG-20 (silica micro-beads, particle size range 20–25 μm), and YWG-35 (silica micro-beads, particle size range 35–40 μm).

The columns used were 10 cm × 2 mm I.D. stainless-steel tubes with smooth inner surfaces, as frequently used in our liquid chromatographic studies[10].

Packing method and preliminary test

In order to ensure packing reproducibility and to obtain highly efficient columns, the columns were packed by the unbalanced-density slurry technique[11], and a carbon tetrachloride–dioxane (2:1, v/v) mixture was used. Then the packed column was conditioned on-line overnight with a flow of pure carrier gas.

According to the Kozeny-Carman and Darcy equation for compressible gas[12], we have

$$\frac{d_p^2 \varepsilon^3}{180(1-\varepsilon)^2} = \frac{2\alpha_0 \eta L}{(p^2-1)p_0} \tag{7}$$

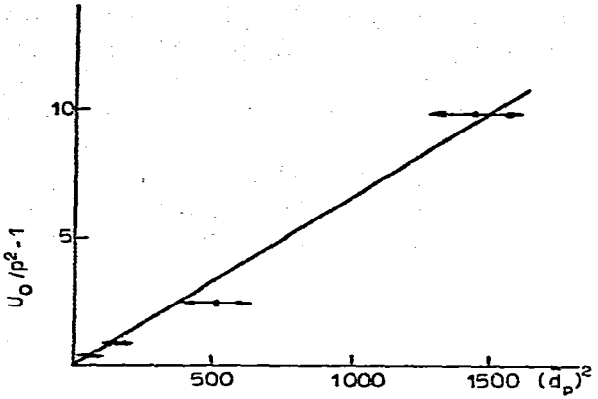

Fig. 1. Plots of U_0/p^2-1 *versus* d_p^2. Temperature, ambient; carrier gas, CO_2.

Hence, as other parameters are constant, such as column dimensions, column temperature and carrier gas, a straight line is obtained when U_0/p^2-1 is plotted against d_p^2, provided that the columns have been packed uniformly. When carbon dioxide was used as the carrier gas, the results in Fig. 1 were obtained.

It can be seen from Fig. 1 that the uniformity of the different columns is sufficiently good to permit further discussion. Improperly packed columns would usually give lower pressure drops than that predicted by eqn. 7.

Signal scanning and sampling

Obviously, the short micro-particle columns have the advantages of both high efficiency and high speed. Sampling and the signal response may play an important role in evaluating column behaviors. In order to obtain a fast signal response, an SC-16 oscilloscope was used to follow the elution peaks. In Fig. 2, the upper curve shows a 100-Hz signal generated by an audiofrequency generator and the lower curve the same signal fed through both an electrometer and a power amplifier, used to follow the output of the FID. By comparing the two recorded curves shown in Fig. 2, it is clear that the deviation from the standard curve (upper curve) can be neglected. The difference between these two curves is only 0.2 cm, while the total peak width at the base of 22 peaks is 21.2 cm.

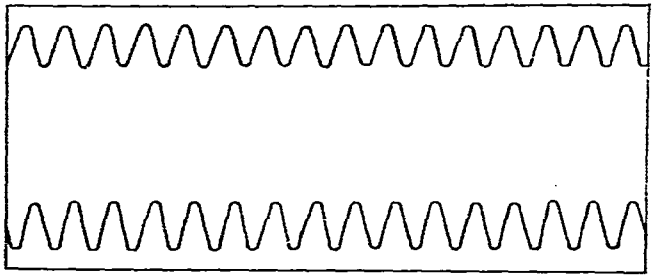

Fig. 2. Rapidly changing signal recorded by SC-16 oscilloscope. Upper curve, oscilloscope coupled directly to frequency generator, 100-Hz signal; lower curve, 100-Hz signal fed through an electrometer and a power amplifier.

The maximum inlet column pressure in this study was 35 kg/cm², when syringe injection was used. From the relationship obtained between the peak width at half-height and the retention time with various carrier gases and different carrier gas velocities as shown in Fig. 3, it was found that the intercept of the plots was less than 0.1 sec in nearly all instances, and all lines almost converged to the same point. It is probable that the extra-column effects are nearly identical in all the experiments.

It was shown earlier[13] that the injection time has only a slight effect on the measurements, provided that the peak width to be measured satisfies the following relation:

$$\Delta t_{\frac{1}{2}} \geqslant 3(\Delta t_{\frac{1}{2}})_{inj} \tag{8}$$

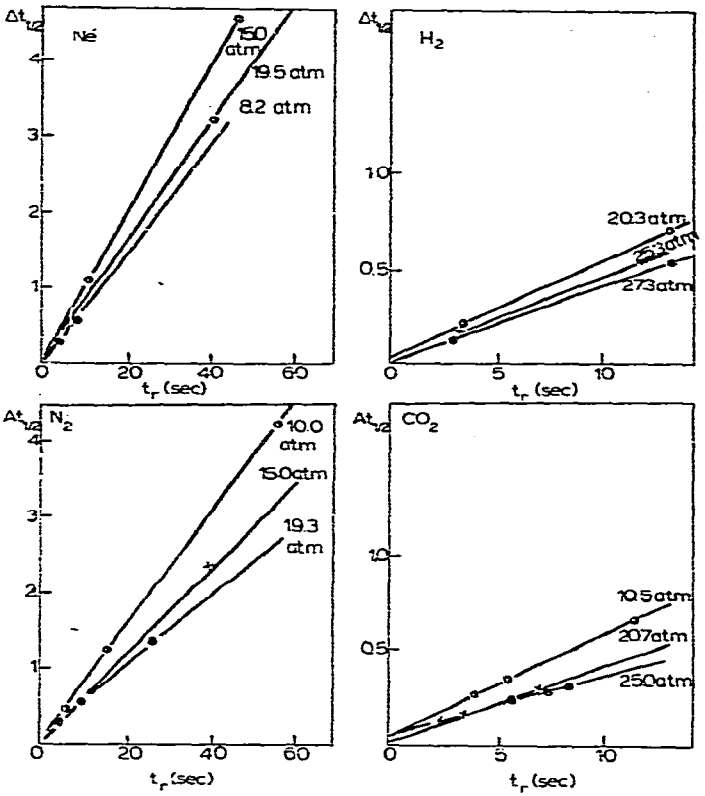

Fig. 3. Relationship between peak width at half-height and retention time for various carrier gases. Column dimensions, 10 cm × 2 mm I.D.; column temperature, ambient; column packing, 7 ± 2 μm silica.

In the limiting case, when $\Delta t_{\frac{1}{2}}$ is equal to $3(\Delta t_{\frac{1}{2}})_{inj}$, the deviation is less than 4%. As the minimal peak width of methane obtained in this study was 0.06 sec, the results obtained with propylene ($k' \approx 3$) in expressing the column efficiency essentially satisfied this requirement.

RESULTS

The results presented below were all obtained at room temperature (25.5 ± 0.5°) with the exception of those specified. Propylene ($k' \approx 3$) was used as a test sample to express the column efficiency in terms of $\bar{H}$ and $\bar{h}$ ($= \bar{H}/\bar{d}_p$). Every experiment was repeated at least five times, the average values being given here.

Effect of mean particle size on column efficiency

Carbon dioxide was used as the carrier gas. The four columns mentioned above were evaluated at various carrier gas velocities. Figs. 4 and 5 give the $\bar{H}$ *versus* $\bar{u}$ and $\bar{h}$ *versus* $\bar{v}$ plots, respectively.

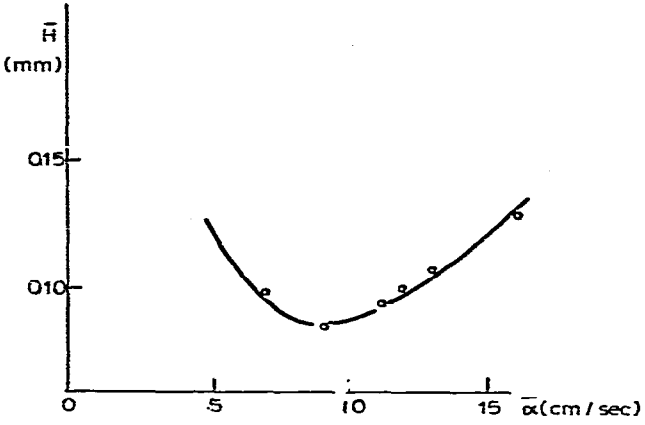

Fig. 4. Plot of $\bar{H}$ against $\bar{u}$. Column dimensions, 10 cm × 2 mm I.D.; column packing, 20–25 μm silica beads.

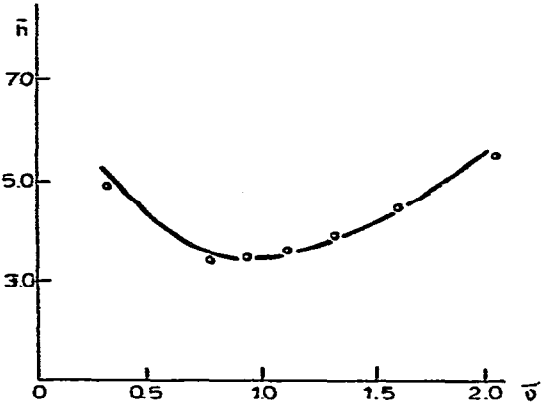

Fig. 5. Plot of $\bar{h}$ against $\bar{v}$. Column conditions as in Fig. 4.

At the optimal linear velocity, each column has the minimal number of theoretical plates ($\bar{H}_{min.}$), and the plot of $\bar{H}_{min.}$ against $\bar{d}_p$ is linear, as shown in Fig. 6.

It can be seen from Fig. 6 that this line, when extrapolated, passes through the origin with a slope of 3.1. It follows that the reduced plate height is 3.1. Some liter-

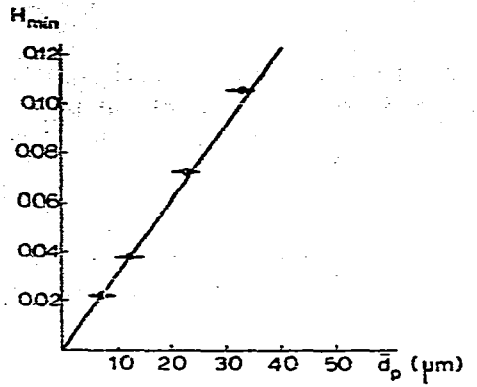

Fig. 6. Plot of $\bar{H}_{min.}$ *versus* $\bar{d}_p$. Carrier gas, CO_2; column temperature, ambient.

TABLE I

SOME VALUES OF $H_{min.}$ IN PACKED COLUMNS

Description	$H_{min.}$	*Number of theoretical plates per metre*	*Reference*
Eqn. 6	$1.6 f_2 d_p$		1
Estimated from equation	$4 d_p$		14
180–200 μm glass beads	$1.7 d_p$		15
180–200 μm Chromosorb W	$5.5 d_p$		15
13 ± 2.9 μm modified alumina beads	$6.4 d_p$	$1.24 \cdot 10^4$	4
30–35 μm modified silica beads	$3.0 d_p$	$1.05 \cdot 10^4$	5
28 μm modified Carbopack C	$3.6 d_p$		7
20–25 μm graphitized carbon black	$2.7 d_p$	$1.70 \cdot 10^4$	8
7 ± 2 μm silica	$3.1 d_p$	$4.5 \cdot 10^4$	
140 μm 405 support	$4.2 d_p$		16
100 μm 6201 support	$4.2 d_p$		1

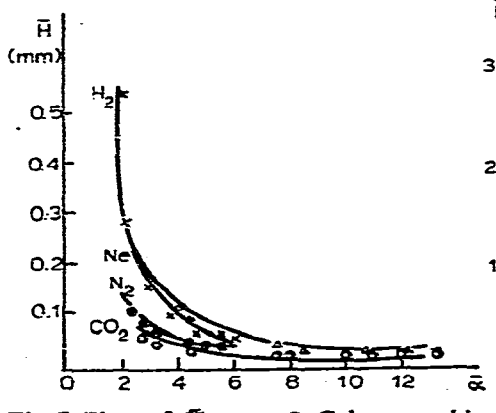

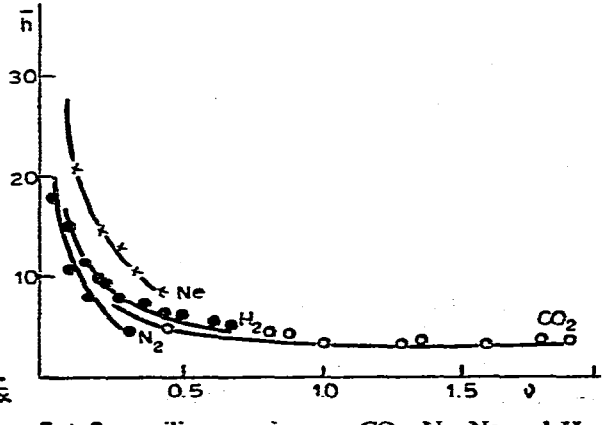

Fig. 7. Plots of $\bar{H}$ *versus* $\bar{\alpha}$. Column packing, 7 ± 2 μm silica; carrier gas, CO_2, N_2, Ne and H_2.

Fig. 8. Plots of $\bar{h}$ *versus* $\bar{\nu}$. Operating conditions as in Fig. 7.

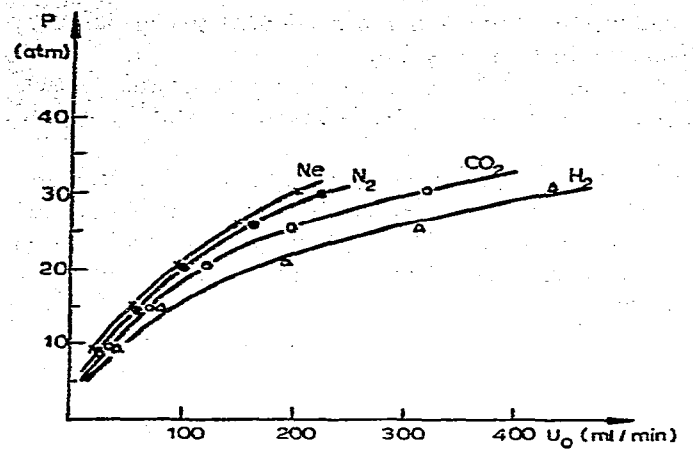

Fig. 9. Effect of column inlet pressure on outlet gas flow-rate for different carrier gases. Column packing, 7 ± 2 μm silica; column temperature, ambient.

ature data are given in Table I. It appears possible that the much larger number of theoretical plates per metre obtained in our work was due to the smaller particle size used.

Effect of mobile phase (carrier gas) on column efficiency

Using 7 ± 2 μm silica as column packing, we studied the effect of different carrier gases and different linear velocities on $\bar{H}$ and $\bar{h}$. Four carrier gases were used, *viz.*, carbon dioxide, nitrogen, neon and hydrogen. Plots of $\bar{H}$ and $\bar{h}$ *versus* $\bar{\alpha}$ and $\bar{\nu}$ are shown in Figs. 7 and 8, respectively.

Because the viscosity of carbon dioxide is smaller than that of nitrogen and neon, it has a much higher flow-rate at the same inlet pressure (see Fig. 9). Further,

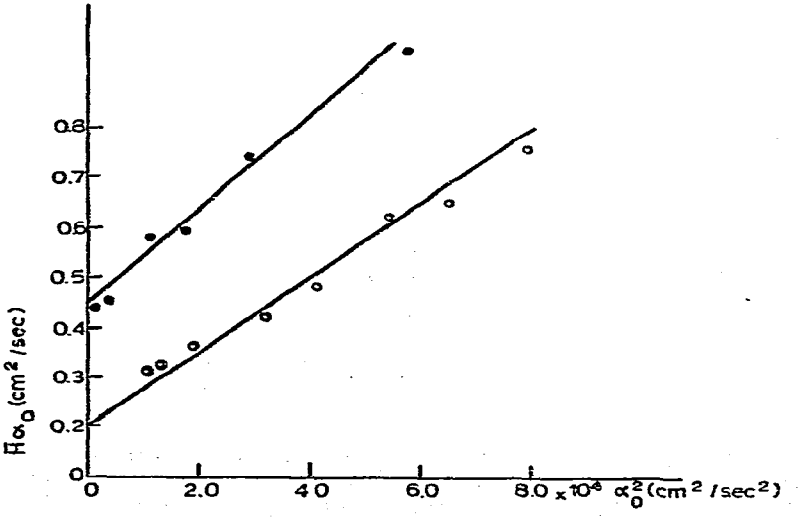

Fig. 10. Plots of $\bar{H}\alpha_0$ *versus* α_0^2. Column packing, 7 ± 2 μm; column temperature, ambient.

owing to its smaller diffusion coefficient, it gives a more efficient performance at relatively low inlet pressures, as shown in Figs. 7 and 8.

On comparing Fig. 5 with Fig. 8, it is also clear that the smaller the particle diameter of the packing, the faster is the mass transfer between the stationary and the mobile phase.

When $\bar{H}\alpha_0$ was plotted against α_0^2 (Fig. 10), straight lines with a correlation coefficient of 0.98 were obtained. The slopes of the two straight lines were calculated by the least-squares method to be $9 \cdot 10^{-6}$ and $8 \cdot 10^{-6}$ sec when hydrogen and carbon dioxide, respectively, were used as the carrier gas. The intercepts of the two lines are smaller than their diffusion coefficients.

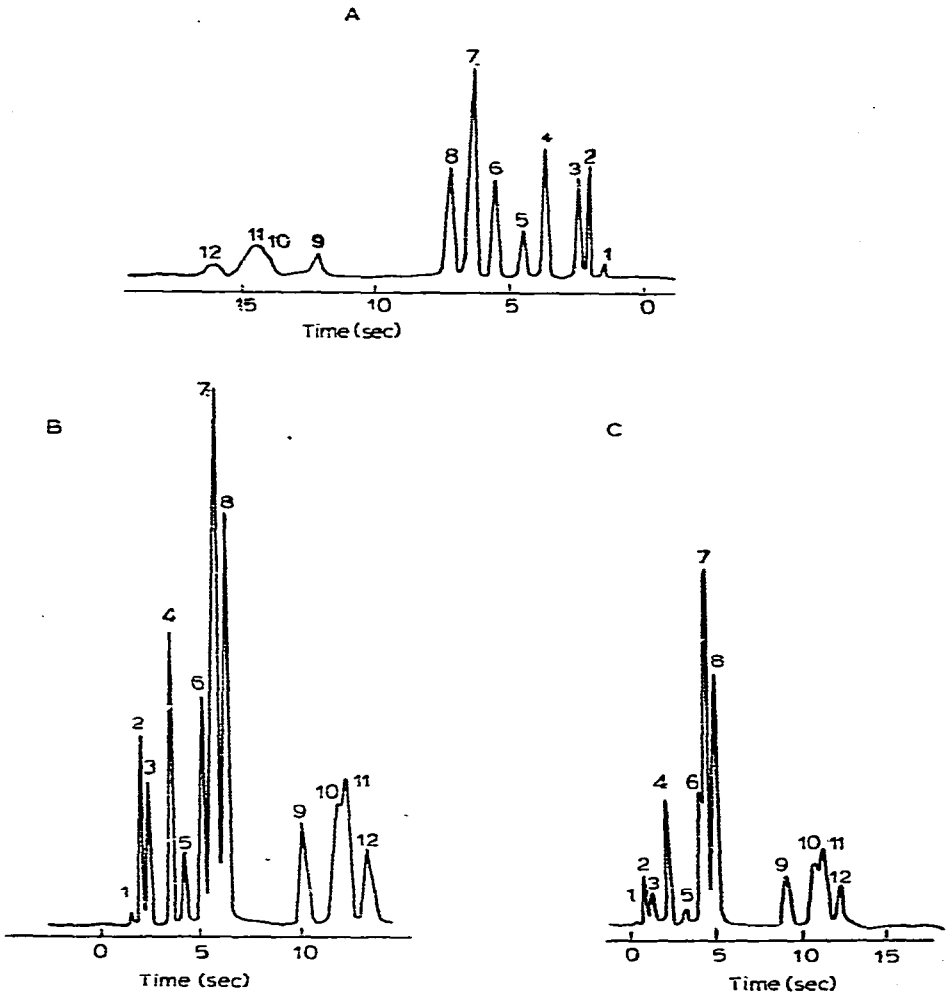

Fig. 11. Separation of gaseous hydrocarbons with carbon dioxide as carrier gas. Column packing, 7 ± 2 μm silica; column temperature, (A) 19°, (B) 30°, (C) 40°. Peaks: 1 = methane; 2 = ethane; 3 = ethylene; 4 = propane; 5 = acetylene; 6 = propylene; 7 = isobutane; 8 = *n*-butane; 9 = butene-1; 10 = *trans*-butene-2; 11 = 1,3-butadiene; 12 = *cis*-butene-2.

Separation of gaseous hydrocarbon mixtures

C_1–C_4 hydrocarbon mixtures were separated on a short (10 cm × 2 mm I.D.) column packed with 7 ± 2 μm silica, using both carbon dioxide and nitrogen as the carrier gas. The results are shown in Figs. 11 and 12. It can be seen that the selectivity of the columns was different when the carrier gas or column temperature was changed.

We can conclude that it is preferable to use carbon dioxide as the carrier gas for the separation of C_1–C_3 hydrocarbons, but for the separation of C_4 hydrocarbon mixtures the better selectivity of nitrogen may be preferred.

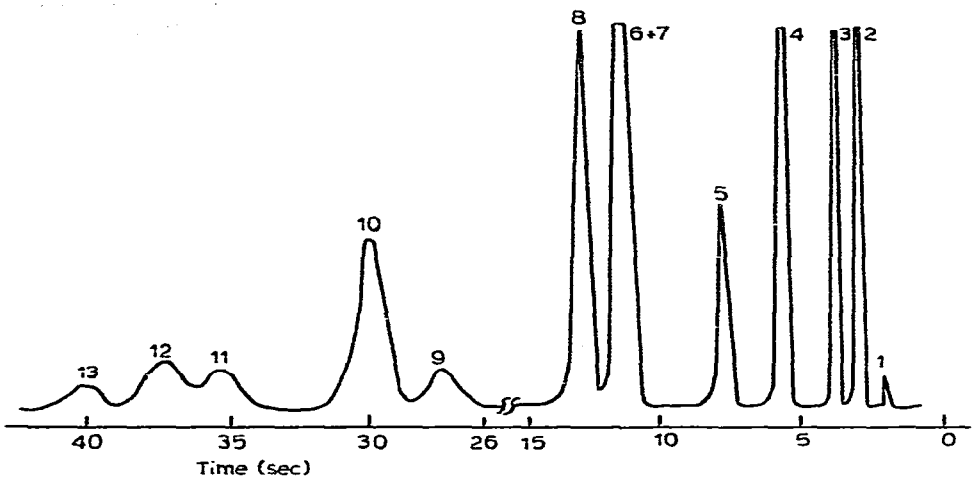

Fig. 12. Separation of gaseous hydrocarbons with nitrogen as carrier gas. Column packing, 7 ± 2 μm silica; column temperature, ambient. Peaks: 1 = methane; 2 = ethane; 3 = ethylene; 4 = propane; 5 = acetylene; 6 = propylene; 7 = isobutane; 8 = *n*-butane; 9 = butene-1; 10 = unknown; 11 = *trans*-butene-2; 12 = 1,3-butadiene; 13 = *cis*-butene-2.

In the separations described, the overall time required for an analysis was less than 20 sec.

DISCUSSION AND CONCLUSION

The optimal result with the high-performance micro-particle gas chromatographic columns, with column dimension of 10 cm × 2 mm I.D., packed with 7 ± 2 μm silica, using carbon dioxide as carrier gas and operating at ambient temperature, was found to be $4.5 \cdot 10^3$ theoretical plates, corresponding to $4.5 \cdot 10^4$ theoretical plates per metre. An overall mass transfer coefficient of less than 10^{-5} sec was obtained. Hence the number of theoretical plates per second for propylene would be better than $1.0 \cdot 10^3$ at higher linear velocities ($\bar{u} > 10$ cm/sec). Twelve gaseous hydrocarbons were separated within about 20 sec under these conditions. According to earlier work[9], the peak capacity of a column is directly determined by the number of theoretical plates of that column. Thus, when a packed column with 4000–5000 theoretical plates is used, one can obtain more then 20 peaks. This should be useful in analysing ordinary samples.

One could anticipate that it will be suitable to use such a short, high-efficiency

column either for performing trace analyses or routine analyses, including process control, in 1 min or less.

The reduced plate height ($\bar{h}$) obtained was 3.1, which is still much higher than that predicted by eqn. 6. The resistance of the interfacial mass transfer may still play a significant role in this instance.

ACKNOWLEDGEMENTS

The authors thank Professor Wang Hongli for fruitful discussions and Mr. Bao Miansheng and Mr. Liang Zuocheng for skilled experimental assistance.

SYMBOLS

d_p	Particle diameter of column packings.
D_l, D_g	Solute diffusion coefficient in liquid and mobile phase, respectively (cm^2/sec).
d_f	Thickness of liquid film.
H	Height equivalent to a theoretical plate (cm).
$H_{min.}$	Minimal value of H.
h	Reduced plate height (H/d_p).
k'	Solute capacity factor.
k	Solute distribution constant.
k_g	Mass transfer coefficient in interfacial phase (cm/sec).
L	Column length (cm).
N	Number of theoretical plates.
P_i	Column inlet pressure.
P_0	Outlet pressure.
p	Ratio of inlet and outlet pressures.
$\Delta t_{\frac{1}{2}}$, $(\Delta t_{\frac{1}{2}})_{inj}$	Peak width at half-height contributed by column and injection, respectively (sec).
t_r	Retention time (sec).
U_C	Carrier gas flow-rate at column outlet (ml/min).
α	Linear velocity (cm/sec).
α_0	Linear velocity reduced at column outlet (cm/sec).
ε'	$1-\varepsilon/\varepsilon$, where ε is the column porosity.
ν	Reduced velocity ($\alpha d_p/D_g$).
σ	Area per volume for mass transfer (1/cm).
λ,β,γ	Related parameter in Van Deemter equation.

The subscript zero denotes values measured at the column outlet, average values are denoted by a bar above a symbol.

REFERENCES

1 Lu Peichang, Zhou Liangmo, Wang Guanghua and Xu Fangbao, unpublished results, 1964.
2 Zhou Liangmo and Lu Peichang, *Sci. Sin.*, 14 (1965) 859.
3 Lu Peichang, Zhou Liangmo and Wang Guanghua, *Thesis*, Chinese University of Science and Technology, Hefei, 1964.

4 M. N. Myers and J. C. Giddings, *Anal. Chem.*, 38 (1966) 294.
5 J. F. K. Huber, H. H. Lauer and H. Poppe, *J. Chromatogr.*, 112 (1975) 377.
6 K. Kenji, *Kagaku No Ryoiki*, 120 (1978) 63.
7 A. Di Corcia and M. Glabbal, *Anal. Chem.*, 50 (1978) 1000.
8 A. Di Corcia, A. Liberti and R. Samperi, *J. Chromatogr.*, 167 (1978) 243.
9 Lu Peichang, *Sci. Sin.*, 22 (1979) 321.
10 Dalian Institute of Chemical Physics, Chinese Academy of Sciences, Group of Liquid Chromatography, unpublished results, 1975.
11 Dalian Institute of Chemical Physics, Chinese Academy of Sciences, Group of Liquid Chromatography, unpublished results, 1975.
12 *Handbook of Gas Chromatography*, (Ed. Group of Chromatography, Berjing Chemical Institute, Chinese Academy of Sciences), Science Press, Berjing, 1977, p. 14.
13 Ding Jingqun, Tang Weixu and Zhu Baolin, unpublished results, 1964.
14 I. Halász, H. Schmidt and P. Vogtel, *J. Chromatogr.*, 126 (1976) 19.
15 C. A. Cramers, J. Rijks and P. Boček, *J. Chromatogr.*, 65 (1972) 29.
16 Dalian Institute of Chemical Physics, Chinese Academy of Sciences, Group of Chromatography, *FenX: Hua Xue*, 3 (1975) 299.